2006 IEEE Int. Conf. on Robotics and Automation, Orlando, FL, 2006.

Stability Analysis of Information Based Control for Biochemical Source Localization

Panos Tzanos and Miloš Žefran
Department of Electrical and Computer Engineering, University of Illinois at Chicago, Chicago, IL 60607, USA
{*ptzano1,mzefran*}*@uic.edu*

***Abstract*— The paper proposes an improved model and its approximation for a diffusion of a biochemical agent in the air. Based on the model, a new motion control algorithm based on the Fisher Information Matrix (FIM) for detecting and localizing a biochemical source is proposed. We show that the location of the biochemical source is an equilibrium point of the system under such control. Simulations with a single moving sensor show that that the biochemical source is located with a high degree of accuracy while the trajectory of the sensor converges to the source.**

I. Introduction

One of the main public safety concerns is the possibility of a biochemical attack [1]. Systems using sensors that can detect low concentration vapors show promise as a means of responding and preventing such attacks. Low concentration vapor sensors have already found use in applications such as landmine detection and localization [2], and the monitoring of the ocean's dynamic physical characteristics and chemical distributions [3]. These sensors also have the potential to be used in other applications such as detection of drugs, sensing leakage of hazardous chemicals, pollution sensing and environmental studies [4].

Due to technological advances in networking and the miniaturization of electromechanical systems, it will be possible in the near future to perform many of the previously mentioned sensing tasks using groups of robots working together through ad-hoc communication networks [5]. However, the coordination algorithms for such mobile sensing networks are difficult to develop since they must conform to the spatially-distributed nature and limited communication capabilities of the network. A different approach to network communication known as distributed or localized networking takes advantage of the physically distributed nature of the sensors by designing coordination algorithms that allow sensor nodes to only communicate with other nodes within some neighborhood. These networks have the advantage that the communication overhead scales well with increases in network size, and they are robust to failure due to the lack of a central data processing node [6].

Considerable work exists on the problem of tracing an odor plume to its source [7]–[11]. A majority of approaches use the concentration gradient to find the source. In [12], an alternative approach was proposed, where the robot moves so that in each step the information that its sensors provide is maximized. The algorithm outperforms concentration gradient based schemes, but it requires more sophisticated modeling and estimation.

Similarly to the approach in [13], we expand on the work of [12] where a single vehicle mounted with vapor sensors is employed to estimate the location of a source emitting vapor at a constant rate in an infinite volume. The vehicle is controlled in real time to reduce as much as possible the expected location estimation error after the next measurement is taken. This is accomplished by computing the gradients of the Cramér-Rao bound (CRB) on the location error with respect to the vehicle's coordinates, and then moving the vehicle in the gradient descent direction. The location estimation is performed using maximum likelihood (ML) estimation. Since ML estimates are asymptotically efficient (their variance approaches the CRB as the data length goes to infinity), it is expected that the actual accuracy of the estimation will be close to the CRB. Hence, by minimizing the CRB the actual estimation error is expected to be minimized. The use of the CRB or Fisher information (the inverse of the CRB) as an optimality criterion for other control problems has been explored in [14] and [15]. Other authors have used Kalman filter estimation [16], or Levenberg-Marquardt optimization [17] for estimating unknown parameters. However, with these methods, there is no guarantee of achieving the lowest possible estimator variance.

The concentration model presented in [12] has a singularity at the vapor source location since the source is assumed to have zero volume. This singularity poses a problem when one tries to find the equilibrium points of any control algorithm used to steer the vehicle. Also, the presence of parameters that we are not interested in, otherwise known as nuisance parameters [18], further complicate our stability analysis. In this paper we first develop a model for a cylindrical source of finite volume. We then present a numerically tractable approximation of this model and a general theory for the stability analysis of a whole family of concentration distributions to which both models belong. Finally, we present a new control algorithm where the negative effects of the nuisance parameters are removed. It is shown through simulation that the trajectory taken by the vehicle with the new control algorithm converges to a limit cycle tightly encircling the vapor source.

II. System Stability

The concentration model used in [12] is the solution to the classic diffusion equation for a source-free volume [19]

$$\frac{\partial c}{\partial t} = \kappa \nabla^2 c \tag{1}$$

where c is the concentration (the dependence of c on time and space has been omitted for convenience) and κ is the diffusivity of the medium, which is assumed to be space invariant. For a point source (zero volume) at $\vec{r}_\circ = [x_\circ, y_\circ]^T$ (we assume the source is located on the ground) in an infinite medium, releasing a diffusing substance at a constant rate of μ, starting at time $t_\circ$, the solution to (1) is given by

$$c(\vec{r},t) = \frac{\mu}{4\pi\kappa|\vec{r}-\vec{r}_\circ|}\,\mathrm{erfc}\left(\frac{|\vec{r}-\vec{r}_\circ|}{2\sqrt{\kappa(t-t_\circ)}}\right) \tag{2}$$

where $\mathrm{erfc}(x) = (2/\sqrt{\pi})\int_x^\infty e^{-y^2}dy$ is the complementary error function. It is worth mentioning that the effects of the wind can be easily included in the model [12]. With the assumption of white Gaussian measurement noise of zero mean and variance σ^2, and a "clutter" term b representing the sensor's response to foreign substances that may be present, we can model the measurements as

$$y(\vec{r},t) = c(\vec{r},t) + b + e(\vec{r},t),\ e(\vec{r},t) \sim \mathcal{N}(0,\sigma^2). \tag{3}$$

We are interested in information based control, so we will use the CRB gradient based control algorithms in our analysis. Namely, we define the dynamics of the system as follows:

$$\begin{aligned} x[n+1] &= x[n] + \mathrm{tr}(\frac{\partial}{\partial x[n+1]}\,\mathrm{CRB}(\vec{r}_\circ)) \\ y[n+1] &= y[n] + \mathrm{tr}(\frac{\partial}{\partial y[n+1]}\,\mathrm{CRB}(\vec{r}_\circ)). \end{aligned} \tag{4}$$

From the results of [12] it appears that $\vec{r} = \vec{r}_\circ$ is an equilibrium point of the system. However, it can be easily seen that the concentration function (2) has a singularity at $\vec{r} = \vec{r}_\circ$. The reason for this singularity is that the source is assumed to have zero volume. The singularity of the concentration function is problematic when one tries to study the stability of control schemes through linearization since the derivative does not exist at $\vec{r}_\circ$. On the other hand, it is clear that in a real-world setting the concentration will be always finite. This motivates finding a solution of (1) for a source with nonzero volume.

The first result we state concerns the conditions under which it is easy to analyze the equilibrium points for a gradient algorithm described above. Namely, a sufficient condition for the vapor source location to be an equilibrium point is that the concentration function is continuously differentiable and of the form

$$f(\vec{r},\vec{r}_\circ,t) = \frac{g(t)}{(|\vec{r}-\vec{r}_\circ|^p + a)} \tag{5}$$

where p and a are constants.

Theorem 1: Let $f(\vec{r},\vec{r}_\circ,\mathrm{t})$ be a continuously differentiable concentration function and of the form given in (5). Suppose the only unknown parameters are the source location parameters $\vec{r}_\circ = [x_\circ, y_\circ]^T$ and σ^2. Then $\vec{r} = \vec{r}_\circ$ is an equilibrium point of the system (4).

Proof: Let us assume that we have maximum likelihood estimates for $\vec{r}_\circ$ and σ^2. Also suppose that we have collected n concentration measurements at n different locations and n equally spaced time instances. We can therefore lump all the measurements into the following vector form:

$$\mathbf{y} = \mathbf{F}(\vec{r}_\circ)\mathbf{x} + \mathbf{e} \tag{6}$$

where $\mathbf{y}$ is an $n\times 1$ dimensional vector whose i-th element is the concentration at position $\vec{r}_i$ and time t_i. $\mathbf{F}(\vec{r}_\circ)$ is an $n\times 2$ dimensional matrix whose i-th row is given by $[f(\vec{r}_i,\vec{r}_\circ,t_i),1]$, and $\mathbf{x}$ is a 2×1 dimensional vector of the form $[m,b]^T$ where m is some known constant. Finally $\mathbf{e}$ is an $n\times 1$ dimensional vector of Gaussian random noise elements.

To find the CRB we must first derive the Fisher information matrix (FIM). The FIM can be viewed as a measure of intrinsic accuracy of a distribution and the CRB is its inverse [20]. The FIM is defined as [21]

$$\mathrm{FIM}(\xi) = -\mathrm{E}\left[\frac{\partial^2 \ln p(\mathbf{y};\xi)}{\partial\xi\partial\xi^T}\right] \tag{7}$$

where $\xi = [\vec{r}_\circ, \sigma^2]^T$ and $p(\mathbf{y};\xi)$ is the probability density function of $\mathbf{y}$ and is

$$p(\mathbf{y};\xi) = \frac{1}{(2\pi\sigma^2)^{n/2}} e^{\frac{-(\mathbf{y}-\mathbf{Fx})^T(\mathbf{y}-\mathbf{Fx})}{2\sigma_e^2}}. \tag{8}$$

Plugging (8) into (7) we get

$$\mathrm{FIM}(\xi) = \frac{1}{\sigma^2}\begin{bmatrix} m^2\mathbf{Q}^T(\vec{r}_\circ)\mathbf{Q}(\vec{r}_\circ) & 0 \\ 0 & n/2\sigma^4 \end{bmatrix} \tag{9}$$

where $\mathbf{Q}(\vec{r}_\circ) = \frac{\partial \mathbf{f}(\vec{r}_\circ)}{\partial \vec{r}_\circ}$ is an $n\times 2$ dimensional matrix of the partial derivative of the first column of $\mathbf{F}(\vec{r}_\circ)$ with respect to the unknown source location. Being that the FIM(ξ) is block diagonal in this case, CRB($\vec{r}_\circ$) is just the inverse of the upper left-hand block,

$$\mathrm{CRB}(\vec{r}_\circ) = \frac{\sigma^2}{m^2}[\mathbf{Q}^T(\vec{r}_\circ)\mathbf{Q}(\vec{r}_\circ)]^{-1}. \tag{10}$$

We now compute the gradient of the CRB with respect to the prospective new position $\vec{r}(n+1) = [x(n+1), y(n+1)]^T$ as done in [12]. Let ζ be any one of the elements of $\vec{r}(n+1)$. Then,

$$\begin{aligned} \frac{\partial}{\partial\zeta}CRB(\vec{r}_\circ) = &-\frac{m^2}{\sigma^2}[\mathbf{Q}^T(\vec{r}_\circ)\mathbf{Q}(\vec{r}_\circ)]^{-1}\cdot \\ &[\frac{\partial\mathbf{Q}^T(\vec{r}_\circ)}{\partial\zeta}\mathbf{Q}(\vec{r}_\circ) + \mathbf{Q}^T(\vec{r}_\circ)\frac{\partial\mathbf{Q}(\vec{r}_\circ)}{\partial\zeta}]\cdot \\ &[\mathbf{Q}^T(\vec{r}_\circ)\mathbf{Q}(\vec{r}_\circ)]^{-1}. \end{aligned} \tag{11}$$

Due to the special from of $f(\vec{r},\vec{r}_\circ,t)$, we can show that the term $\frac{\partial\mathbf{Q}^T(\vec{r}_\circ)}{\partial\zeta}\mathbf{Q}(\vec{r}_\circ)$, and likewise its transpose, go to zero since it has the form

$$\begin{bmatrix} 0 & \dots & 0 & \times \\ 0 & \dots & 0 & \times \end{bmatrix}\cdot \begin{bmatrix} & \times & & \times \\ & \vdots & & \vdots \\ & \times & & \times \\ \frac{-pg(t)(x-x_\circ)|\vec{r}-\vec{r}_\circ|^{p-2}}{(|\vec{r}-\vec{r}_\circ|^p-a)^2} & & \frac{-pg(t)(y-y_\circ)|\vec{r}-\vec{r}_\circ|^{p-2}}{(|\vec{r}-\vec{r}_\circ|^p-a)^2} & \end{bmatrix} \tag{12}$$

which is zero when $\vec{r} = \vec{r}_\circ$. Thus the whole gradient matrix is zero. ■

The decoupled structure of the FIM matrix is very important. Without it, it would add extra complexity to the inversion of the FIM and in most cases we would not be able to determine if the system has any equilibrium points. Also, a close examination of the above argument shows that it is actually not necessary that the concentration function has the form (5), all that is needed is that the it has a maximum at $\vec{r} = \vec{r}_\circ$.

III. The Modified FIM Motion Algorithm

In light of the results of the previous section, we propose a new information based algorithm for controlling the sensor mounted vehicle.

In [13], the concentration model used had a singularity at the source location, due to the fact that the authors used a point source which has zero volume. In reality, chemical sources have a finite volume or surface area. However for a circular disk source – which can be seen as a generalization of the point source – there is no analytical solution for the concentration function [19]:

$$c(r,t) = \begin{cases} \int_0^t \frac{\mu}{\pi a^2}(1 - e^{\frac{-a^2}{4\kappa(t-t')}})dt', & \text{if } r = 0, \\ \int_0^t \int_0^a \frac{\mu}{2\kappa\pi a^2} \frac{e^{\frac{-(r^2-r'^2)}{4\kappa(t-t')}}}{t-t'} I_\circ(\frac{rr'}{2\kappa(t-t')}) r' dr' dt' \end{cases} \tag{13}$$

where a is the radius of the disk, $I_\circ$ is a Bessel function of the second kind and of order zero, and it is assumed that $t_0 = 0$ for simplicity. As in [12], it is easy to also model the effects of the wind.

We thus start by assuming the following measurement model for a source releasing vapor at a constant rate

$$y(\vec{r},t) = \frac{\mu(1 + e^{-\kappa(t-t_\circ)})}{1 + |\vec{r} - \vec{r}_\circ|^2} + b + e(\vec{r},t), \qquad e(\vec{r},t) \sim \mathcal{N}(0,\sigma^2) \tag{14}$$

where the unknown parameters are the initial time $t_\circ$, the source location $\vec{r}_\circ$, the clutter b, the noise variance σ^2 and the constants μ and κ which can respectively be thought of as having the same effects as the release rate and diffusivity constant of a true concentration function. We chose the model in (14) due to the fact that its features match those of the concentration function for a circular disk source. In particular, both functions have a maximum at the source location so Theorem 1 applies. A comparison of the one dimensional cross-sections of the concentration distribution for a circular disk source and our analytical model in the steady state is shown in Figure 1.

Assuming that we have taken n measurements at n different locations and at n equally spaced time instances, we can collect all of the measurements into the following vector form

$$\mathbf{y} = \mathbf{F}(\theta)\mathbf{x} + \mathbf{e} \tag{15}$$

which is similar to (6) except now the matrix $\mathbf{F}(\theta)$ contains the unknown parameters $\theta = [\vec{r}_\circ, \kappa, t_\circ]^T$ and $\mathbf{x}$=$[\mu, b]^T$.

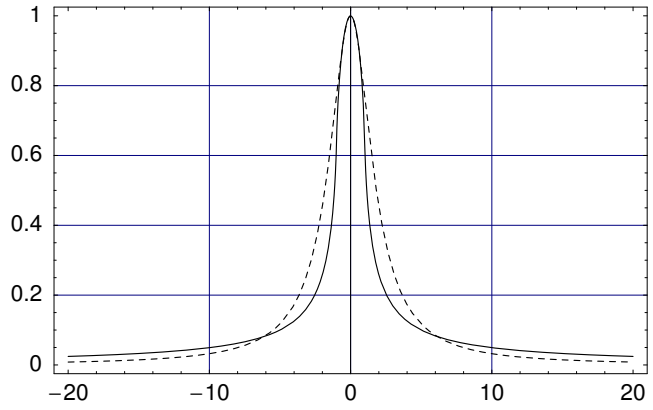

Fig. 1. A one dimensional cross-section of the concentration functions given by Eq. (13) (solid) and Eq. (14) (dashed) in steady state.

A. Parameter Estimation

As in [12], [13] we estimate the unknown parameters $\Psi = [\vec{r}_\circ, \kappa, t_\circ, \mu, b, \sigma^2]^T$ using ML estimation. The maximum likelihood estimates $\hat{\theta}$, $\widehat{\mathbf{x}}$, and $\hat{\sigma}_e^2$ maximize the joint probability density function of the measurements (the *likelihood function*), $\widehat{\Psi} = \arg\max_\Psi L(\mathbf{y}|\Psi)$ [22]. The likelihood function is given by

$$L(\mathbf{y}|\Psi) = \frac{1}{(2\pi\sigma^2)^{n/2}} e^{\frac{-(\mathbf{y}-\mathbf{F}(\theta)\mathbf{x})^T(\mathbf{y}-\mathbf{F}(\theta)\mathbf{x})}{2\sigma_e^2}}. \tag{16}$$

The maximum likelihood estimates are [4]

$$\hat{\theta} = \arg\max_\theta \{\mathbf{y}^T P_{\mathbf{F}}(\theta)\mathbf{y}\} \tag{17}$$

$$\widehat{\mathbf{x}} = [\mathbf{F}^T(\hat{\theta})\mathbf{F}(\hat{\theta})]^{-1}\mathbf{F}^T(\hat{\theta})\mathbf{y} \tag{18}$$

$$\hat{\sigma}_e^2 = (mp)^{-1}\mathbf{y}^T P_{\mathbf{F}}^\perp(\hat{\theta})\mathbf{y} \tag{19}$$

where $P_{\mathbf{F}}(\theta)$ is the projection matrix onto the column space of $\mathbf{F}(\theta)$,

$$P_{\mathbf{F}}(\theta) = \mathbf{F}(\theta)[\mathbf{F}^T(\theta)\mathbf{F}(\theta)]^{-1}\mathbf{F}^T(\theta), \tag{20}$$

and $P_{\mathbf{F}}^\perp(\theta) = I - P_{\mathbf{F}}(\theta)$ is the complementary projection matrix. From equation (17) it can be seen that the ML estimate $\hat{\theta}$ is the θ that maximizes the projection of the column space of $\mathbf{F}(\theta)$ onto the data vector $\mathbf{y}$ and vice versa.

The Cramér-Rao bound for unbiased estimates of the parameters are

$$\text{CRB}(\theta) = \frac{\sigma^2}{\mu^2}\mathbf{Q}^T(\theta)P_{\mathbf{F}}^\perp(\theta)\mathbf{Q}(\theta) \tag{21}$$

$$\text{CRB}(\mathbf{x}) = \sigma^2\{\mathbf{F}^T(\theta)[\mathbf{I} - \mu^2 P_{\mathbf{Q}}(\theta)]\mathbf{F}(\theta)\}^{-1} \tag{22}$$

$$\text{CRB}(\sigma^2) = \frac{2\sigma^4}{n} \tag{23}$$

where $\mathbf{Q}(\theta) = \frac{\partial \mathbf{f}(\theta)}{\partial \theta}$, the partial derivative of the first column of $\mathbf{F}(\theta)$ with respect to θ, which is an $n \times 4$ dimensional matrix. These are derived in detail in [23].

B. Motion Algorithm

We now propose our new motion algorithm. Suppose a single sensor has taken n measurements at n known locations and instants. Assume the measurements were taken periodically with the period T so that the time to take n measurements is nT. With these n measurements, an estimate $[\hat{x}_{on}, \hat{y}_{on}]^T$ of the source coordinates can be obtained with the algorithm described in the previous subsection. The accuracy of these estimates can be estimated from the Cramér-Rao lower bound if we assume that the algorithm is statistically efficient (or the variances of the estimates are a small multiple of the bound, if we allow for relative efficiency) [21]. While the CRB depends on the unknown parameters θ so it can not be computed, an estimate of the CRB can be obtained by substituting the current estimates for all unknown parameters. Denote the coordinates of the sensor after the nth measurement as $\vec{r}(nT) = [x(nT), y(nT)]^T$, and let $\mathcal{S}_{n+1}$ be the set of all points reachable by the sensor at time $(n+1)T$, given the speed, maneuvering limitations, and geometrical constraints. Compute the FIM which has the following form:

$$\text{FIM}(\Psi) = \frac{1}{\sigma^2}\begin{bmatrix} \mu^2\mathbf{Q}^T(\theta)\mathbf{Q}(\theta) & \mu\mathbf{Q}^T(\theta)\mathbf{F}(\theta) & 0 \\ \mu\mathbf{F}^T(\theta)\mathbf{Q}(\theta) & \mathbf{F}^T(\theta)\mathbf{F}(\theta) & 0 \\ 0 & 0 & \frac{n}{2\sigma^2} \end{bmatrix}. \tag{24}$$

For a general parameter vector ξ, we may partition the parameter space as $\xi = [\xi_1, \xi_2]^T$ where ξ_1 is a vector containing the parameters of interest, and ξ_2 is a vector containing all nuisance parameters. Then, with the probability density function $p(\mathbf{y};\xi)$ given, the FIM(ξ) has the following structure:

$$\text{FIM}(\xi) = \begin{bmatrix} -E[\frac{\partial^2 \ln p(\mathbf{y};\xi)}{\partial\xi_1\partial\xi_1^T}] & -E[\frac{\partial^2 \ln p(\mathbf{y};\xi)}{\partial\xi_1\partial\xi_2^T}] \\ -E[\frac{\partial^2 \ln p(\mathbf{y};\xi)}{\partial\xi_2\partial\xi_1^T}] & -E[\frac{\partial^2 \ln p(\mathbf{y};\xi)}{\partial\xi_2\partial\xi_2^T}] \end{bmatrix}. \tag{25}$$

Using the formula for inverting block matrices [21], CRB(ξ_1) is

$$\begin{aligned} CRB(\xi_1) = (&-E[\frac{\partial^2 \ln p(\mathbf{y};\xi)}{\partial\xi_1\partial\xi_1^T}]+ \\ &E[\frac{\partial^2 \ln p(\mathbf{y};\xi)}{\partial\xi_1\partial\xi_2^T}]E[\frac{\partial^2 \ln p(\mathbf{y};\xi)}{\partial\xi_2\partial\xi_2^T}]^{-1}E[\frac{\partial^2 \ln p(\mathbf{y};\xi)}{\partial\xi_2\partial\xi_1^T}])^{-1}. \end{aligned} \tag{26}$$

As can be seen from equation (26), using the true CRB for motion control adds extra complexity to the stability analysis since it involves terms related to the nuisance parameters which have no bearing on the motion of the sensor. For this reason, we will devise a motion algorithm based on the upper left-hand block of FIM(Ψ).

Notice that the upper left-hand block has the same form as the upper left-hand block in equation (9). Therefore, if we compute the gradient of the inverse of the upper left-hand block after $n+1$ measurements, and move the sensor in the opposite direction to the gradient we are guaranteed to have an equilibrium point at the source location. Going through the same process as in equation (11), the gradient is found to be

$$\begin{aligned} \frac{\partial}{\partial\zeta}\frac{\mu^2}{\sigma^2}[\mathbf{Q}^T(\theta)\mathbf{Q}(\theta)]^{-1} = &-\frac{\mu^2}{\sigma^2}[\mathbf{Q}^T(\theta)\mathbf{Q}(\theta)]^{-1}\cdot \\ &[\frac{\partial\mathbf{Q}^T(\theta)}{\partial\zeta}\mathbf{Q}(\theta) + \mathbf{Q}^T(\theta)\frac{\partial\mathbf{Q}(\theta)}{\partial\zeta}]\cdot \\ &[\mathbf{Q}^T(\theta)\mathbf{Q}(\theta)]^{-1}. \end{aligned} \tag{27}$$

To determine the direction of motion of the sensor, we must devise a scalar criterion. Since the gradient will be zero at the source location no matter which elements we choose, we have chosen the trace of the matrix. Unfortunately, since the matrix $\mathbf{Q}(\theta)$ depends on the history of the sensors motion, it is not possible to determine analytically through linearization the stability properties of the equilibrium point at the vapor source. In our future work we plan to address this question through the analysis of the FIM.

This algorithm can be extended to the multiple moving sensor case very easily. Using a distributed network, all sensors transmit to their neighbors their current concentration measurement. A neighbor can be considered to be any sensor within a given communication radius for example. Each sensor then computes their own ML estimates and employs the modified FIM motion algorithm to determine its next location. Once that location is reached, each sensor determines who its new neighbors are, and then repeats the process.

IV. Results

In this section we employ the modified FIM gradient algorithm for the case of a single sensor. A vapor emitting source is placed at the coordinates (-50,-50)m. The constants μ and κ are set at 1 and .005 respectively. A bias of $10^{-4}Kg/m^3$ and zero-mean Gaussian noise with standard deviation, $\sigma = 10^{-7}Kg/m^3$ are considered to be present in the measurements. The emission of vapor begins $100s$ before any measurements are taken. Beginning at $t = 100s$ the vehicle starts moving along a circular path with a radius of $250m$ centered at (0,0) at a speed of $5m/s$ and collects measurements every $10s$. This is done so that there is a spatially diverse set of measurements to begin ML estimation with.

The detection of the vapor is assumed to have occurred at $t = 400s$ and the modified FIM gradient algorithm begins, using the measurements obtained while traversing the circle. In this phase, the vehicle moves at a maximum speed of $1m/s$, and a line search algorithm is employed to find the minimum along the direction of the gradient up to the maximum distance the vehicle can travel, which is $10m$. When the vehicle is closer than $5m$ from the source the sensor always moves 1/4 the distance to the source in the direction of the gradient. This is all done so that we can illustrate a smooth trajectory and the limit cycle. Figure 2(a) illustrates the movement of the sensor. The sensor first moves in a straight line in the general direction of the source, and then begins to circle around the source, obtaining spatially diverse measurements that help in pinpointing the exact location of the source. On a large scale, these results

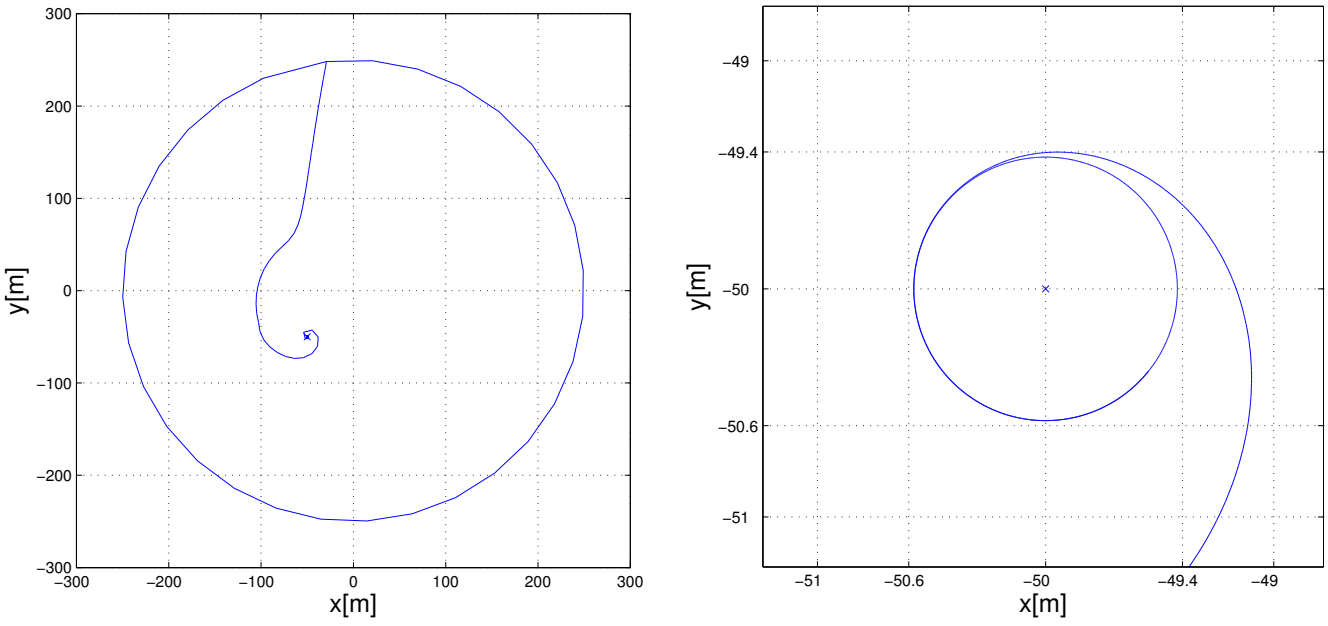

(a) The sensor's path.

(b) A view of the limit cycle.

Fig. 2. AN example of the trajectory of the sensor under the proposed motion algorithm. The source, denoted with an "x", is located at (-50,-50).

are quite similar to the ones in [12] where the Direction of Gradient (DOG) algorithm was employed, but Figure 2(b) shows that the trajectory of the vehicle converges to a limit cycle encircling the source rather than the source itself. The limit cycle is a perfect circle, centered at the vapor source location, and has a radius of about $.6m$. However, a further analysis reveals that the limit cycle is actually the artifact of the approximation (14) and does not occur if the exact model (13) is used.

The CRB estimates (or more precisely, the square root of the estimates) corresponding to the source location estimates are presented in Figure 3(b). The simulation was allowed to run until each CRB estimate dropped below $10^{-10}m^2$. This was achieved after 1664 times steps, or $16640s$. Finally the source location estimates are shown in Figure 3(a). The estimates converge to the correct location, and achieve convergence after about 40 time steps ($400s$).

V. Conclusion

In this paper we showed that for a broad class of concentration functions and a block diagonal CRB matrix, an equilibrium point for CRB-gradient based control systems can be found, and it is the location of the vapor source. We applied this result to devise a new gradient based motion algorithm, the modified FIM motion algorithm, and showed that we are able to correctly locate the vapor source with high accuracy. Finally we showed through simulations that the motion trajectory of the mobile sensor converges to the vapor source. In our future work we plan to apply the new motion algorithm to a distributed network of sensors. It would also be worthwhile to investigate this algorithm's performance in a real environment, taking into account factors such as wind, obstacles and biochemical sensor response time.

Acknowledgment

We would like to thank Prof. Arye Nehorai for the insightful discussions that led to this work. This research is supported in part by NSF grants IIS-0093581 and CCR-0330342.

References

[1] J. Fitch, E. Raber, and D. Imbro, "Technology challenges in responding to biological or chemical attacks in the civilian sector," *Science*, vol. 32, pp. 1350–1354, Nov. 2003.

[2] A. Jeremić and A. Nehorai, "Landmine detection and localization using chemical sensor array processing," *IEEE Trans. Signal Processing*, vol. 48, no. 5, pp. 1295–1305, May 2000.

[3] E. Kaltenbacher, R. Byrne, and E. Steimle, "Design and applications of a chemical sensor compatible with autonomous ocean-sampling networks," *IEEE J. Oceanic Eng.*, vol. 26, no. 4, pp. 667–670, Oct. 2001.

[4] A. Nehorai, B. Porat, and E. Paldi, "Detection and localization of vapor-emitting sources," *IEEE Trans. Signal Processing*, vol. 43, no. 1, pp. 243–253, Jan. 1995.

[5] J. Cortés, S. Martínez, T. Karatas, and F. Bullo, "Coverage control for mobile sensing networks," *IEEE Trans. Robotics and Automation*, vol. 20, no. 2, pp. 243–255, Apr. 2004.

[6] D. Estrin, R. Govindan, J. Heidemann, and S. Kumar, "Next century challenges: scalable coordination in sensor networks," in *Proceedings of the Fifth Annual International Conference on Mobile Computing and Networks*, Aug. 1999.

[7] H. Ishida, T. Nakamoto, and T. Morizumi, "Remote sensing of gas/odor source location and concentration distribution using mobile system," *Sensors and actuators B*, vol. 49, no. 1-2, pp. 52–57, 1998.

[8] S. Kazadi, R. Goodman, D. Tsikata, D. Green, and H. Lin, "An autonomous water vapor plume tracking robot using passive resistive polymer sensors," *Autonomous robots*, vol. 9, no. 2, pp. 175–188, 2000.

[9] F. W. Grasso, "Invertebrate-inspired sensory-motor systems and autonomous, olfactory-guided exploration," *Biological bulletin*, vol. 200, no. 2, pp. 160–168, 2001.

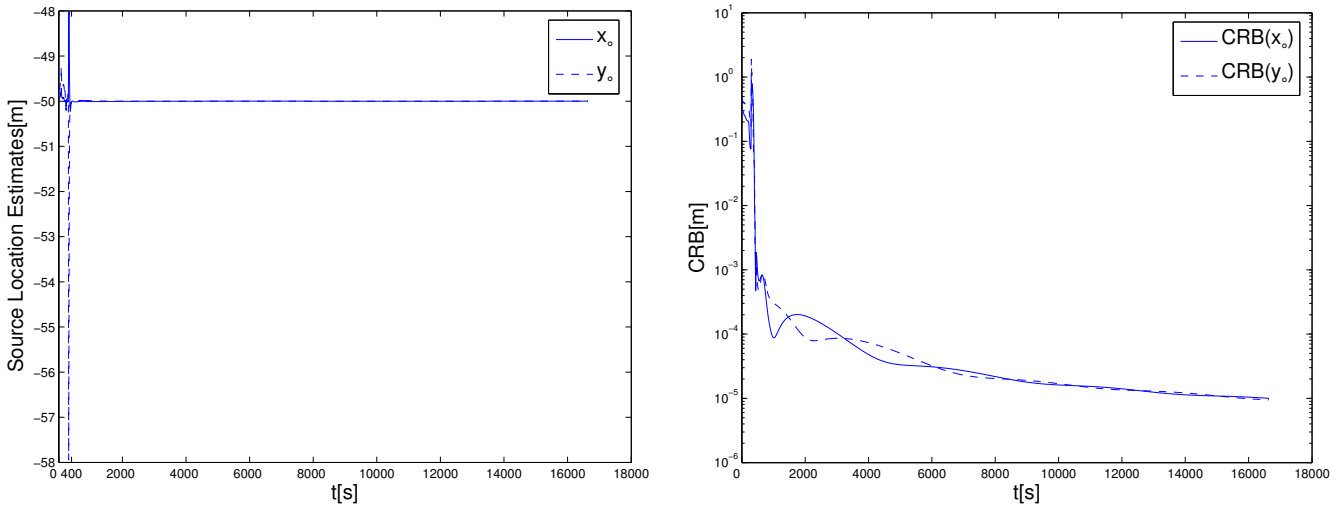

(a) The source location estimates.

(b) Square root of the estimate of the Cramér-Rao bound.

Fig. 3. An example of estimation performance of the proposed algorithm.

[10] R. A. Russell, "Survey of robotic applications for odor-sensing technology," *International Journal of Robotics Research*, vol. 20, no. 2, pp. 144–162, 2001.

[11] L. Marques, U. Nunes, and A. de Almeida, "Olfaction-based mobile robot navigation," *Thin solid films*, vol. 418, no. 1, pp. 51–58, 2002.

[12] B. Porat and A. Nehorai, "Localizing vapor-emitting sources by moving sensors," *IEEE Trans. Signal Processing*, vol. 44, no. 4, pp. 1018–1021, Apr. 1996.

[13] P. Tzanos, M. Žefran, and A. Nehorai, "Information based distributed control for biochemical source detection and localization," in *Proceedings of the 2005 IEEE International Conference on Robotics and Automation*, Apr. 2005, pp. 4468–4473.

[14] J. Helferty and D. Mudgett, "Optimal observer trajectories for bearings-only tracking by minimizing the trace of the crámer-rao lower bound," in *Proceedings of the 32nd Conference on Decision and Control*, Dec. 1993, pp. 936–939.

[15] D. Uciński, "Optimal sensor location for parameter estimation of distributed processes," *Int. J. of Control*, vol. 73, no. 13, pp. 1235–1248, 2000.

[16] T. Chung, V. Gupta, J. Burdick, and R. Murray, "On a decentralized active sensing strategy using mobile sensor platforms in a network," in *43rd IEEE Conference on Decision and Control*, Dec. 2004, pp. 1914–1919.

[17] V. Christopoulos and S. Roumeliotis, "Adaptive sensing for instantaneous gas release parameter estimation," in *Proceedings of the 2005 IEEE International Conference on Robotics and Automation*, Apr. 2005, pp. 4461–4467.

[18] M. Moeneclaey, "On the true and the modified cramer-rao bounds for the estimation of a scalar parameter in the presence of nuisance parameters," *IEEE Trans. Communications*, vol. 46, no. 11, pp. 1536–1544, Nov. 1998.

[19] J. Crank, *The Mathematics of Diffusion*. Oxford University Press, 1956.

[20] C. Rao, *Linear Statistical Inference and its Applications*. New York: Wiley, 1973.

[21] S. M. Kay, *Fundamentals of Statistical Signal Processing: Estimation Theory*. Upper Saddle River, NJ: Prentice Hall, 1993.

[22] H. Stark and J. W. Woods, *Probability, Random Processes, and Estimation Theory for Engineers*. Upper Saddle River, NJ: Prentice Hall, 1994.

[23] P. Stoica and A. Nehorai, "MUSIC, maximum likelihood, and Cramér-Rao bound," *IEEE Trans. Acoust., Speech, Signal Processing*, vol. 37, no. 5, pp. 720–741, May 1989.